



University of Connecticut
OpenCommons@UConn

Master's Theses

University of Connecticut Graduate School

2-27-2013

Monitoring MDPC-23 Odontoblast-Like Cell Proliferation Using Cell Count and DNA Content Methods

Marina Funtik D.M.D.

University of Connecticut School of Dental Medicine, Prosthodontics, funtikmarina@hotmail.com

Recommended Citation

Funtik, Marina D.M.D., "Monitoring MDPC-23 Odontoblast-Like Cell Proliferation Using Cell Count and DNA Content Methods" (2013). *Master's Theses*. 389.
https://opencommons.uconn.edu/gs_theses/389

This work is brought to you for free and open access by the University of Connecticut Graduate School at OpenCommons@UConn. It has been accepted for inclusion in Master's Theses by an authorized administrator of OpenCommons@UConn. For more information, please contact opencommons@uconn.edu.

Monitoring MDPC-23 Odontoblast-Like Cell Proliferation Using Cell Count and DNA Content Methods

Marina Funtik

B.S., St. Lawrence University, 2005

D.M.D., University of Connecticut School of Dental Medicine, 2009

A Thesis

Submitted in Partial Fulfillment of the

Requirements for the Degree of

Master of Dental Science

At the

University of Connecticut

2013

APPROVAL PAGE

Master of Dental Science Thesis

Monitoring MDPC-23 Odontoblast-Like Cell Proliferation Using Cell Count and
DNA Content Methods

Presented by

Marina Funtik, D.M.D.

Major Advisor _____

A. Jon Goldberg, Ph. D.

Associate Advisor _____

Liisa T. Kuhn, Ph. D.

Associate Advisor _____

John R. Agar, D.D.S., M.A.

University of Connecticut

2013

Acknowledgements

A Special Thank You to Dr. Cheryl Gomillion for her utmost attention to detail, steadfast guidance and in-depth knowledge that helped this project be a wonderful and fun learning experience.

Table of Contents

1.0	Introduction.....	1
1.1	Dental Caries: Current Therapies and Challenges	1
1.2	Regeneration of Physiological Dentin (Insert clinical image where this could be used)...	5
1.3	Odontoblast Cell Line	6
1.4	Growth Curves	7
2.0	Hypotheses	9
3.0	Specific Aims.....	10
4.0	Materials and Methods:.....	11
4.1	Preparation of Cell Cultures	11
4.2	MDPC-23 Cell Counts, Growth Curves and Doubling Time	11
4.3	DNA Quantification of the MDPC-23 Cell Cultures Using Quant-iT™ dsDNA Reagent 13	
4.4	DNA Standard Curves.....	14
4.5	DNA from MDPC-23 cells	15
5.0	Results:.....	17
6.0	Discussion	27
7.0	Conclusion	31
	Appendix 1	35
	Appendix 2.....	36

Abstract

There is growing interest in the development of an engineering process by which dentin stem/progenitor cells can predictably proliferate, differentiate and produce mineralization nodules in cell culture. The engineering of 3D scaffolds could then be used to aid in proliferation and differentiation of these progenitor cells to aid in regeneration of the pulp/dentin complex *in vivo*.

In the present study, the goal was to characterize the MDPC-23 cell line and its behavior during proliferation. The cells in culture reach high numbers upon reaching confluence. When cells are growing in multilayers, as will occur in planned dentin regeneration experiments, it is difficult to accurately establish the cell number. DNA content can be used to determine cell number, but the correlation between cell number and DNA content for MDPC-23 cells needs to be validated.

We designed three experiments to establish growth curves and cell doubling time for the MDPC-23 cell line and finally to correlate cell numbers to DNA content in the MDPC-23 cell line. In the initial experiment to characterize cell growth, MDPC-23 cells number was plotted over a time period of 11 days. In the second experiment MDPC-23 cell growth was monitored for 11, with cell numbers counted manually using a hemocytometer. The cells from each time point were also used to measure the DNA content using fluorescence. The third experiment had more refined methods using a TC10™ automatic cell counter and then plotting these numbers to obtain the MDPC-23 growth curve. The cells were also used for DNA content calculation using the same dilution factor of 80x for all DNA samples.

The cell doubling times for two MDPC-23 cell cultures in Experiment #1 were 1.02 days and 1.12 days. In Experiment #2 the MDPC-23 cell doubling time was 0.94 days and for Experiment #3 it was 0.90 days. The average cell doubling time for all three experiments was 0.996 ± 0.095 days.

The cell numbers and DNA content in Experiment #2 were not closely correlated (correlation coefficient of $R^2 = 0.875$). The cell numbers and DNA content for Experiment #3 were closely correlated with a correlation coefficient of $R^2 = 0.98$.

The MDPC-23 cell line has a typical S-shaped growth curve. This study confirmed the null hypothesis that MDPC-23 cell numbers as determined by cell counting closely correlate to DNA content.

1.0 Introduction

1.1 Dental Caries: Current Therapies and Challenges

Dental caries remains the most common chronic disease of children and the elderly in both developing and industrialized countries (Cardeiro et al. 2008, Petersen et al. 2005).

According to the World Health Organization, oral health is still a major public health problem worldwide (Petersen 2008, Wang et al. 2010). Pain and loss of productivity at school and work are sequellae of untreated dental caries (tooth decay). The most common treatment of dental caries involves mechanical removal of affected dental tissues, enamel and dentin, and placement of direct dental restorations (amalgam fillings, resin composite fillings, porcelain inlays or onlays). If the carious lesion is advanced, in some situations pulp capping is the treatment of choice. Pulp capping is an alternative procedure to root canal treatment that preserves the vitality of potentially infected pulp tissue using chemicals such as calcium hydroxide, mineral trioxide aggregate (MTA) or beta tricalcium phosphate (TCP).

The longevity of dental restorations has been extensively studied (Goldberg et al., 2006). Microleakage and degradation of restorative materials over time are just some of the problems arising from these procedures (Tonomura et al., 2010). Bacterial infiltration due to microleakage can lead to more problems including inflammation, infection and secondary caries (Tonomura et al., 2010). These synthetic materials erode and degrade over time and mechanically do not match the natural tooth structure they are replacing, leading to additional problems.

Novel research has been focusing on regeneration of dental tissues as an alternative to traditional restorative treatments. Regeneration of dental pulp tissue has been the focus of many previous studies (Balic et al. 2009, Balic et al. 2005, Cardeiro et al. 2008). However, study of

dentin regeneration has not been extensive, even though dentin comprises the greatest amount of tooth structure and would have a potentially significant impact on dental treatment. Even when experimentally successful, dentin regeneration produced dentin that was not physiologically normal (tubular) dentin.

Physiological tubular dentin matrix is secreted by elongated odontoblasts (Mina et al. 2004). Odontoblasts, located at the periphery of dental pulp, are highly specialized tall columnar cells secreting dentin. Dentin, the most abundant tooth tissue, is composed of mostly mineral but also contains collagen and noncollagenous proteins. Dentin phosphoprotein (DPP) and dentin sialoprotein (DSP) are noncollagenous proteins involved in dentin formation and mineralization (Liu et al. 2006). Type I collagen is a major constituent of the organic matrix of dentin (86-90%) (Mina et al. 2004). Collagen provides a scaffold for mineralization, while noncollagenous proteins initiate and regulate the process of mineralization (Liu et al. 2006).

Postmitotic odontoblasts are dentin-secreting cells that remain active throughout the life of the tooth and secrete primary and secondary dentin (dentin formed after completion of root formation). While dentin is unable to undergo remodeling, odontoblasts are capable of responding to an injury (Mina et al. 2004). If the damage is reversible and odontoblasts survive they secrete *reactionary (tertiary)* dentin. If the damage is irreversible, odontoblasts are replaced by a second generation of odontoblast-like cells that secrete atubular *reparative dentin matrix (osteodentin)* (Mina et al. 2004, Tziafas 2004, Sloan et al. 2009).

One approach to utilizing regeneration in dentistry is seen with deciduous tooth pulpotomies. Pulpotomy is indicated to prevent premature loss of the primary tooth by removing only the coronal aspect of pulp tissue while preserving the pulp in the roots. It is performed in carious primary teeth with normal pulp or teeth with reversible pulpitis or after traumatic pulp

exposure (Srinivasan et al. 2011). For decades, the gold standard for pulpotomy treatment has been formocresol. Formocresol, due to its high toxicity and potential carcinogenicity, has been potentially linked to nasopharyngeal cancer, nasal and paranasal sinus carcinoma and also leukemia in humans (Srinivasan et al 2011). Formocresol has no reparative ability and acts as a fixative. Thus, formocresol is being replaced with materials that have the potential to stimulate regeneration, like mineral trioxide aggregate (MTA) to treat deciduous teeth.

MTA has been indicated for pulp capping, pulpotomy and root end closures and approved by the FDA for use in endodontics in 1998 (Roberts et al., 2008). MTA, first introduced in 1993 by Torabinejaad, is derived from Portland cement. It is a mixture of refined Portland cement and bismuth oxide, which gives it opacity, and contains trace amounts of SiO_2 , CaO , MgO , K_2SO_4 , Na_2SO_4 . Portland cement contains dicalcium silicate, tricalcium silicate, tricalcium aluminate, gypsum and tetracalcium aluminoferrite. MTA in deciduous teeth has been shown to stimulate cytokine release from bone cells, actively promoting hard tissue formation rather than being inert while maintaining integrity of pulp (Srinivasan et al 2011). Clinical applications today include: pulp capping in primary teeth, pulpotomy dressing in primary and permanent teeth, root-end filling material for apicoectomy, root repair material during root perforations, repair of horizontal root fractures, external and internal root resorption repair and apexification/apexogenesis of primary teeth.

The mechanism of action of MTA is induction of alkaline phosphatase, osteonidogen, osteonectin, osteocalcin, and osteopontin in odontoblasts, which results in hard tissue bridge formation. MTA has been shown to initiate hard tissue formation within 2 weeks with minimal inflammation (Guyen et al. 2011). MTA supports healing of the pulp by protection and providing calcium ions necessary for mineralization (Guyen et al. 2011). MTA is thought to also induce

dentin regeneration by inducing periodontal fibroblasts to secrete BMP-2 and TGF- β 1 (Güven et al. 2011). Currently available on the market are ProRoot MTA (Dentsply Endodontics, Tulsa, OK, USA) and MTA Angelus (Srinivasan et al 2011). Even though the results with MTA are encouraging, there are still questions about its effectiveness in regeneration. This is another area where regeneration of dental tissues could be useful.

The most widely used direct restorations are resin composites. Regeneration of dental tissues could also be useful as an alternative or a supplement to the widely used direct restorative materials, such as resin composites. This class of materials is not ideal as resin composites degrade in the oral cavity over time (Hashimoto et al., 2000). Their durability is dependent on the stability of the resin-dentin bond. In the *in vivo* study by Hashimoto, the resin-dentin bond was investigated after aging in the oral environment for 1, 2 or 3 years. Not only was the degradation of resin composite present, but also collagen fibril depletion was observed among aged specimens (Hashimoto et al., 2000). Today, there are many adhesive systems present in dentistry that are either etch-and-rinse or self-etch based. They all rely on micromechanical interlocking of composite material with collagen fibrils of dentin. But dentin-resin bond has not been durable due to the presence of endogenous collagenolytic enzymes called matrix metalloproteinases (MMPs) that are fossilized within the mineralized dentin and can be released and activated during bonding procedures (Tay and Pashley 2004). This hydrolytic degradation of the resin-collagen hybrid layer has been shown to occur in the absence of salivary and bacterial enzymes (Tay and Pashley 2004). To prevent this from occurring, 0.2% chlorhexidine solution has been used to inhibit MMP-2, MMP-8 and MMP-9 (Tay and Pashley 2004). It has been further shown that pre-treatment of the tooth preparation with chlorhexidine prior to implementation of etch-and-rinse technique could preserve collagen fibrils within the hybrid

layer (Tay and Pashley 2004). Dentin regeneration might also be able to address concerns with dentin bonding.

1.2 Regeneration of Physiological Dentin

One necessary goal of dentin regeneration research is to create a biomaterial scaffold with odontoblast inductive properties that could be placed in excavated carious tooth preparations to promote regeneration of tubular dentin in sufficient volume in order to reduce or eliminate the need for traditional restorative materials (fillings) while maintaining tooth vitality and health.



Figure 1: Class I defective resin composite restoration tooth #31 with all 4 walls that would benefit from *in vivo* tubular dentin regeneration.

The formation of tubular regenerative dentin by odontoblast-like cells derived from progenitor cells is influenced by the geometric architecture of the supporting scaffold matrix and the chemistry of functional groups bound to the scaffold. One category of the synthetic scaffolds that could be considered is based on polylactic acid polymers. These scaffolds will need to be evaluated *in vitro* using a well-characterized odontoblast cell line or primary cells. The regenerative scaffold placed into the tooth preparation would modulate dentin regeneration. This could then be considered a permanent restoration with the benefits of avoiding more invasive

dental procedures like root canals and crowns. Partial regeneration would also be possible to ensure a more conservative preparation for a smaller restoration preserving more tooth structure. This regenerative dentistry would completely change the way dentistry is practiced. As with any new treatment, case selection would be critical starting with smaller cavities and then progressing to investigate the effectiveness and efficacy of this bioengineering in dentistry in larger cavities and ultimately on a larger scale.

1.3 Odontoblast Cell Line

One cell type that could be used in the *in vitro* evaluation of scaffolds for dentin regeneration is the immortalized odontoblast-like cell line MDPC-23. It was originally derived from 18-19 day old CD-1 fetal mouse molar dental papillae. The cells have been described previously to be epithelioid with processes and are capable of expressing and secreting dentin sialoprotein (DSP) and dentin phosphoprotein (DPP) in culture (Hanks et al. 1998).

The use of a cell line offers a pure population of odontoblast-like cells that would behave in a consistent manner in culture, whereas with a primary cell population, particularly from the dental pulp, cells may differentiate to odontoblasts as well as osteoblasts, making it difficult to distinguish which cells are responsible for differentiation and subsequent mineral production. The MDPC-23 cell line has many advantages for the present application; it has been used in many studies, it is readily available and immortalized. While these cells are an immortalized population, they do not consistently express odontogenic genes/proteins in culture.

Dentin Sialophosphoprotein (DSPP) is an odontoblast-specific gene that codes for two proteins, dentin sialoprotein (DSP) and dentin phosphoprotein (DPP). DSPP is also expressed in bone, although in much lower quantities. It plays a critical role during dentinogenesis and formation of predentin matrix. If after induction, there is increased DSPP expression, one can

confirm ability of the cell culture to differentiate (Dissanyaka et al. 2011). The products of differentiation of odontoblast cells are mineralization nodules.

In a more recent study of the MDPC-23 cell line by Rodriguez et al. (2009), it was found that DSP expression was not induced in an *in vitro* environment. *In vivo* conditions of mouse-implanted diffusion chamber showed positive expression of DSP. These are special cells that have morphological and phenotypic characteristics of differentiated odontoblasts and express DSP *in vivo*. In diffusion chamber *in vivo* experiments, MDPC-23 cells expressed DSP in addition to type I collagen, osteocalcin and osteopontin (Rodriguez et al., 2009). These findings are very useful to fully characterize the behavior of the MDPC-23 cell line to be able to apply it in dentin regeneration experiments *in vivo*.

1.4 Growth Curves

An initial step in the characterization of a cell line for use in the evaluation of tissue engineering scaffolds would be generation and characterization of its growth curve. The growth curve allows calculation of lag time and cell doubling time. In eukaryotic cells, the cell cycle has 4 stages: S and M phase and preparatory G1 and G2 phases. DNA is replicated during the S phase. During the M phase replicated chromosomes are segregated into 2 daughter nuclei via mitosis. G1 precedes the S phase, and G2 precedes the M phase. During these preparatory phases cellular components necessary to complete the upcoming phase are replicated. They can have varying time lengths, and Tc (cell doubling time) depends on G1 length as it accounts for the difference in Tc between different cell types or between the same cells growing under different conditions (Andreeff et al. 2000).

The proliferation rates depend on three parameters: 1. Rate of cell division/ cell doubling time (T_c), 2. Fraction of cells undergoing division in the given cell population, and 3. Cell death and cell loss due to terminal differentiation.

Cells growing in culture have 3 stages: Lag Phase, Log phase and Plateau Phase (Figure 2). Lag phase usually lasts only a few days, with little increase in cell numbers. Here, cells are undergoing enzyme and cytoskeletal changes. In the Log phase, cell numbers increase exponentially provided critical cell media and nutrition are plentiful. Cells eventually plateau during the last phase where cell numbers remain constant. In monolayer culture, cells cease to divide when they reach confluency demonstrating contact inhibition.

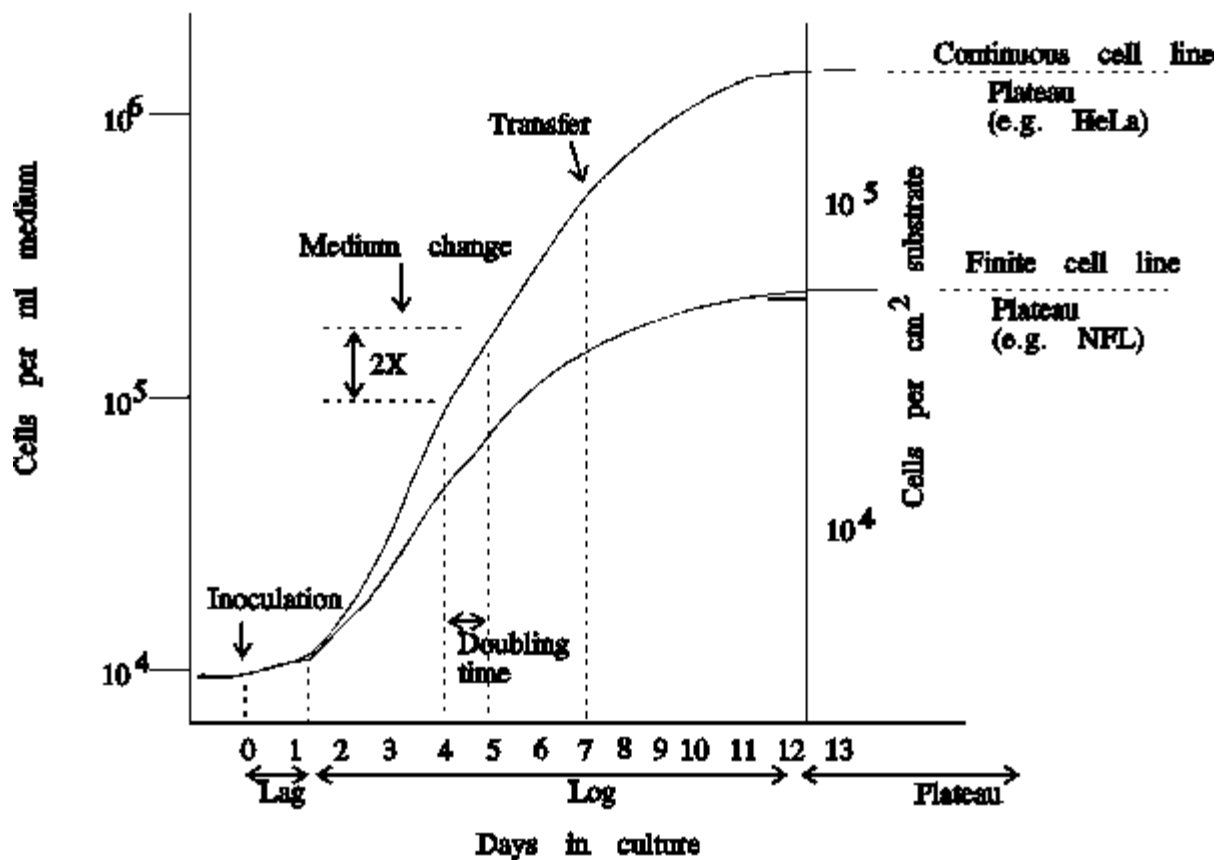


Figure 2: Eukaryotic Cell Growth Curve as adopted from Dr. William H Heidcamp, Gustavus Adolphus College, St. Peter, MN Laboratory Manual

Determining the growth curve for the MDPC-23 cell line is a very important step to fully characterize this cell line and its behavior during the proliferation phase before proceeding to differentiation and mineral production experiments.

As cells proliferate in cell culture the accurate cell numbers are more difficult to obtain as cells become confluent and become multilayer cell culture. This becomes a serious problem with tissue engineering applications where a large volume of cells will be grown in 3D scaffolds. Traditional cell counting methods will not work. Therefore, it is necessary to validate an alternative method to traditional cell counting. DNA content could be a valid approach for calculating cell numbers in multilayer cell culture.

2.0 Hypotheses

The null hypothesis:

During proliferation of MDPC-23 cells, cell number and DNA content are highly correlated and therefore, DNA content could be used as a measure of proliferation when cell number cannot be determined.

3.0 Specific Aims

The aim of this study is to characterize the MDPC-23 murine odontoblast cell line by measuring proliferation in anticipation of further tissue engineering experiments.

This initial project will characterize MDPC-23 murine odontoblast stem cell line by plotting and then evaluating growth curves of the cell line and also calculating cell doubling time. The growth curve plotted from counting cell numbers will then be correlated to growth curves determined by DNA content to validate use of DNA content as a measure of cell number.

Once established, this correlation will be used in future experiments of 2D and 3D models of odontoblasts and various scaffolds for tissue engineering (Appendix 2). Proliferation will be related to differentiation and mineralization in these experiments. The future work will assess cell differentiation in 2-D topographic models by varying chemistry and architecture of scaffolds and evaluating mineral production during differentiation experiments (Appendix 2).

This type of dental research is needed to fully understand the behavior of odontoblast-like cells *in vitro*, to subsequently develop clinically meaningful regenerative *in-vivo* treatment modalities.

4.0 Materials and Methods:

4.1 Preparation of Cell Cultures

The MDPC-23 cells (courtesy of Dr. Hanks and Dr. Nor from University of Michigan, Ann Arbor, MI) were thawed and cultured in proliferation medium containing Dulbecco's Modified Eagles Medium (DMEM, Gibco, Invitrogen) supplemented with 10% heat-inactivated fetal bovine serum (FBS) (HyClone, Logan), 100 units/ml penicillin and 100 ug/ml streptomycin (GIBCO, Invitrogen Corp., Carlsbad, CA, USA) and maintained in a humidified atmosphere of 5% CO₂ and 95% air at 37°C. The cells were maintained at University of Connecticut Dr. Mina Mina's lab in collaboration with Ms. Barbara Rogers.

The cells were maintained in a large petri dish using proliferation media. The medium was changed every 2 days and the cultures were split every 3 – 4 days, the time they reached near confluence. The old media was suctioned out with a sterile pipette, and the cells were rinsed with 10ml of PBS solution to remove any non-adherent cells. PBS solution (pH 7.4 1X , Gibco by Life Technologies) was removed and 1ml of 0.05%- trypsin-0.5mM EDTA was used to detach all attached cells by incubating them for 2 min at 5% CO₂ and 95% air at 37°C. The cells were rinsed with 3ml proliferation media, spun for 3min at 1200 rpms in a centrifuge (Centra CL3R IEC, 24°C, 215 Rotor). The cell pellet was then re-suspended in 1ml of proliferation media. Diluted cells (1:120 dilution [83ul]) were re-suspended into 10ml of fresh media. The cell suspension was then dispensed into a new petri dish. All procedures were conducted in a sterile reverse air flow hood.

4.2 MDPC-23 Cell Counts, Growth Curves and Doubling Time

The project involved three (3) separate experiments: 1. Initial experiment establishing initial MDPC-23 growth curves 2. Second experiment relating growth curves to DNA content using MDPC-23 cells with manual cell counting and then correlating cell numbers and DNA

content, and 3. Third experiment relating growth curves to DNA using a standard dilution and an automatic cell counter and then correlating these cell numbers to DNA content.

The initial experiment entailed counting cell numbers during the proliferation stage of MDPC-23 cells from Day 1-Day 11 of the experiment and comparing two growth curves on both linear and logarithmic scales. In the second and third experiments, in addition to the MDPC-23 growth curves established by counting cell numbers, DNA content was measured and correlated to cell numbers.

In each experiment, MDPC-23 cells were plated onto tissue culture plastic (TCP) 6-well plates (BD Falcon, Fisher) in triplicate at a density of $15,000 \text{ cell/cm}^2$ and incubated at 37°C and $5\% \text{ CO}_2$. The cells for all experiments were seeded with 14.25×10^4 cells in each well of the 6 well plate for each data point. The data points were as follows: Day 0 (seeding day), Day 1, Day 3, Day 4, Day 5, Day 6, Day 7, Day 9 and Day 11. The proliferation medium was changed daily. The DNA content cell samples were frozen at -80°C and DNA content analysis was completed at the end of the whole experiment when all samples were available.

To count the cells the old media was suctioned out with a sterile pipette, and the cells were gently rinsed with 10ml PBS solution to remove any non-adherent cells. PBS solution was suctioned and 1ml of 0.05% trypsin-0.5 mM EDTA was used to detach all attached cells by incubating them for 2 min in $5\% \text{ CO}_2$ and $95\% \text{ air}$ at 37°C . The cells were diluted in proliferation media in the a proper dilution and counted using a hemocytometer.

To count the cells, 100ul of cells in suspension were removed and added into a sterile Eppendorf tube. Trypan blue 100ul was added and mixed gently. Then, 10 ul of the mixture was placed on a clean and dry hemocytometer beneath the coverslip. The cells counts were obtained

for each of the 4 squares. In the last experiment (Experiment #3, passage 2), cells were counted using a TC10™ Automatic Cell Counter (BioRad).

The number of cells/ml was obtained using the following formula:

$$\frac{\text{\# of cells counted} \times 2 \text{ (dilution factor)} \times 10^4}{4 \text{ (number of squares used)}}$$

The total number of cells was then calculated by multiplying the number of cells per ml of suspension and then multiplying it with the total volume of the cell suspension.

Cell doubling time is calculated by using the general formula that describes the cell growth:

$$A = A_0 2^n$$

where A is the number of cells at any time, and A_0 is the initial cell number and n is the number of cell divisions that have taken place.

The value of n can also be described as:

$$n = T/T_c$$

where T is elapsed time and T_c is the doubling time of the cell.

By taking the natural log of both sides, one can solve for the T_c (cell doubling time) by using the following formula:

$$T_c = 0.5T / \log (A/A_0)$$

4.3 DNA Quantification of the MDPC-23 Cell Cultures Using Quant-iT™ dsDNA Reagent

The Quant-IT™ PicoGreen reagent is an ultrasensitive fluorescent nucleic acid stain that quantifies double stranded DNA (dsDNA) in solution with 400-fold higher sensitivity when

compared to the gold standard Hoechst 33258-based assay. The PicoGreen method uses standard spectrofluorometer and fluorescein excitation and emission wavelengths (excitation at 485nm, fluorescence emission at 520nm). Using a fluorescence microplate reader, this assay can detect as little as 250pg/ml dsDNA (50pg in 200uL assay volume). This assay minimizes contributions of RNA and single stranded DNA (ssDNA) to the fluorescence (Invitrogen Molecular Probes Quant-iT™ PicoGreen Reagent Manual). All samples of cells for DNA quantification were prepared in triplicates, including samples of DNA standards.

4.4 DNA Standard Curves

DNA standard curves are used to determine the concentration of DNA in the cells based on the absorbance at 260nm (A_{260}). Usually, for the standard DNA, bacteriophage lambda or calf thymus DNA is used and then diluted in Tris-EDTA (TE) buffer to obtain a working solution with a concentration of 2ug/ml.

Table 1: Preparation of DNA Standard Curve Samples.

Volume (ul) of TE buffer	Volume (ul) of 2ug/ml DNA stock	Volume (ul) of diluted Quant-iT™ PicoGreen Reagent	Final DNA concentration in Quant-iT™ PicoGreen Assay
0	1,000	1,000	1ug/ml
900	100	1,000	100ng/ml
990	10	1,000	10ng/ml
999	1	1,000	1ng/ml
1,000	0	1,000	blank

All 5 DNA standard samples (100ul each) were loaded into a 96-well plate reader and 100ul of Quant-iT™ PicoGreen® reagent was added and incubated at room temperature for 2-5

min. Readings were performed using fluorescence microplate reader (SpectraMax Gemini EM by Molecular Devices). Fluorescence values of the reagent blank were subtracted from each of the five DNA standard samples and corrected values were then plotted to generate five point DNA standard curves of the relative fluorescence versus DNA concentration for both experiments #2 and #3, Figures 7 and 13, respectively.

4.5 DNA from MDPC-23 cells

To prepare MDPC-23 cell samples for DNA analysis, Papain Digestion Solution was prepared as follows: 50mM phosphate buffered solution stock (pH 7.4), 2mM N-acetyl-L-cysteine, 5mM EDTA, and 25ul/ml papain. Papain Digestion Solution was added to each well containing cell samples (1ml per well of 12 well plate) for each data point: Day 1, Day 3, Day 4, Day 5, Day 6, Day 7, Day 9 and Day 11. Samples were incubated at room temperature for 10 min.

Using a sterile scraper, all cells were scraped from each well surface and using a pipette tip, samples were transferred into pre-labeled 2ml microcentrifuge tubes. Samples were then incubated overnight in a water bath at 65°C.

On the following day, the PicoGreen kit was warmed up to room temperature for 15 min. A 20X stock TE (10mM Tris-HCL, 1mM EDTA, pH 7.5) buffer was diluted to 1X TE buffer with sterile, distilled, DNase-free water. The 1X TE buffer was then used to dilute the PicoGreen reagent and DNA samples.

To prepare the Quant-iT™ PicoGreen Reagent Working Solution, a 200-fold dilution of concentrated DMSO solution was obtained by diluting concentrated DMSO in TE buffer and covering it with foil to prevent photodegradation. The diluted DMSO was later added to each well sample in the amount of 100ul. However, for the samples Day 6, Day 7, Day 9 and Day 11,

a 20 X dilution of samples and their standards was used in experiment #2 to ensure that DNA concentrations in all samples were within the upper limits of the standard DNA curves thus ensuring a more accurate measure of DNA content. Exceedingly high DNA concentration in samples could negatively affect the fluorescence measurements. In experiment #3, all samples (Day 1- Day 11) were diluted with same dilution factor (80X) to ensure equal treatment of all samples in the experiment.

Sample analysis was then performed by pipetting 100ul of the sample DNA solutions in TE 1X buffer into a well of a 96 well plate (Corning Incorporated, Corning, NY), then 100ul of Quant-iT™ PicoGreen Reagent was added to a final volume of 200ul and incubated for 5 min at room temperature protected from light. The fluorescence of the samples and standards was then measured. The fluorescence value of the reagent blank was then subtracted from each of the samples. DNA concentration of the samples was then determined from the DNA Standard Curve.

5.0 Results:

The growth curves in the initial Experiment #1 (culture #1 and #2) were plotted for linear and log models. They were both typical S-shaped curves. Linear and logarithmic sale growth curves for Experiment #1 were plotted as shown in Figures 3 and 4, respectively.

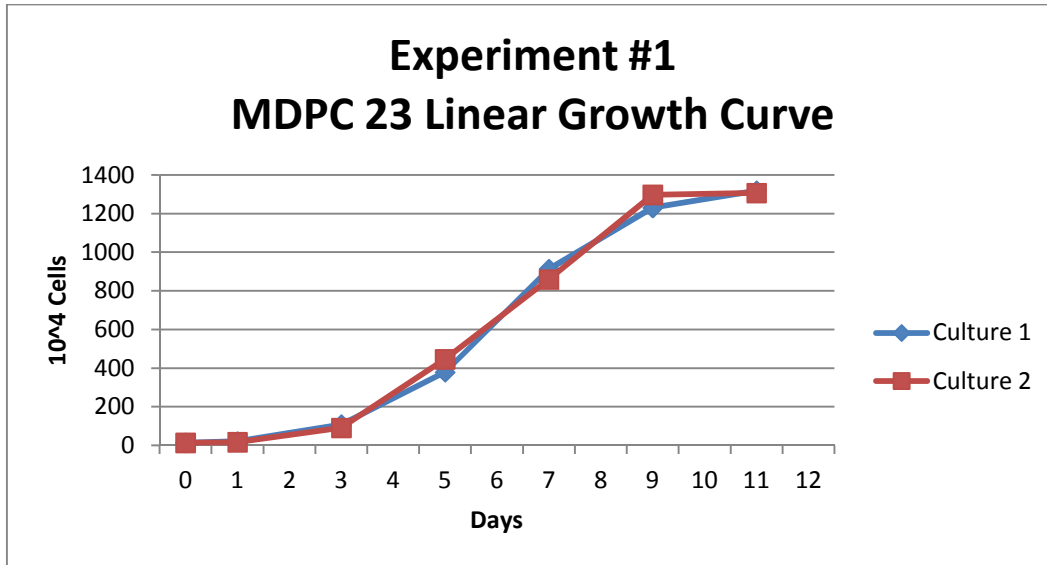


Figure 3: Experiment #1 MDPC-23 linear growth curve during 11 days in cell culture, culture #1 and #2.

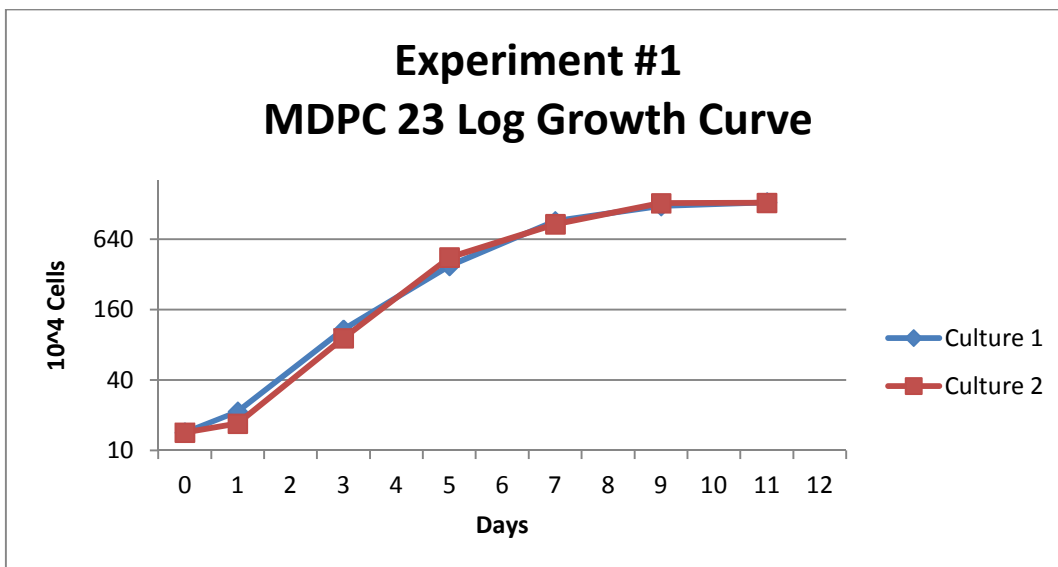


Figure 4: Experiment #1 MDPC-23 cell log growth curve during 11 days in cell culture, culture #1 and #2.

From the linear growth curve, cell doubling time (T_c) was calculated as shown in Table 2 below for 1st experiment MDPC-23 Culture #1, where cell doubling time (T_c) was determined to be 1.02 days (Table 2).

<p>Cell doubling time (T_c)</p> $T_c = 0.3 \times T / (\log A/A_0)$ $= 0.3 \times 3 / \log (108/14.25)$ $= 0.9/\log 7.57$ $= 1.02 \text{ days}$	<p>A - # of cells at any time</p> <p>A_0 - # of cells at time T</p> <p>T – elapsed time</p> <p>T_c- cell doubling time</p>
---	--

Table 2: MDPC-23 cell doubling time (T_c) calculation.

Cell doubling time has been calculated for each of the three experiments. The cell doubling time for MDPC-23 Experiment #1 growth curve was 1.02 days for Culture #1 and 1.12 days for Culture #2. For Experiment #2, cell doubling time was 0.94 days and for Experiment #3 was 0.90 days. These were then averaged and with an average cell doubling time of 0.996 +/- 0.095 days.

In Experiment #2 MDPC-23 cell numbers were counted and correlated to DNA content. The plotted cell numbers produced a growth curve that was not uniformly S-shaped. This could be due to dilutions during the counting being different for all data points (Figures 5 and 6). The log growth curve for Experiment #2 was more consistent with the shape of a typical growth curve (Figure 6). All MDPC-23 cells were manually counted using a hemocytometer and Trypan blue stain.

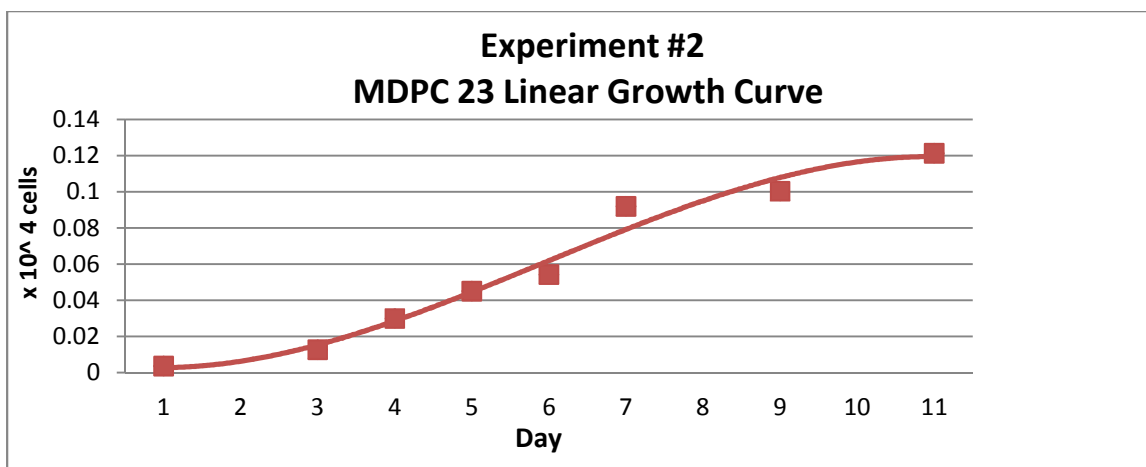


Figure 5: Experiment #2 MDPC-23 cell linear growth curve during 11 days in cell culture manually counted.

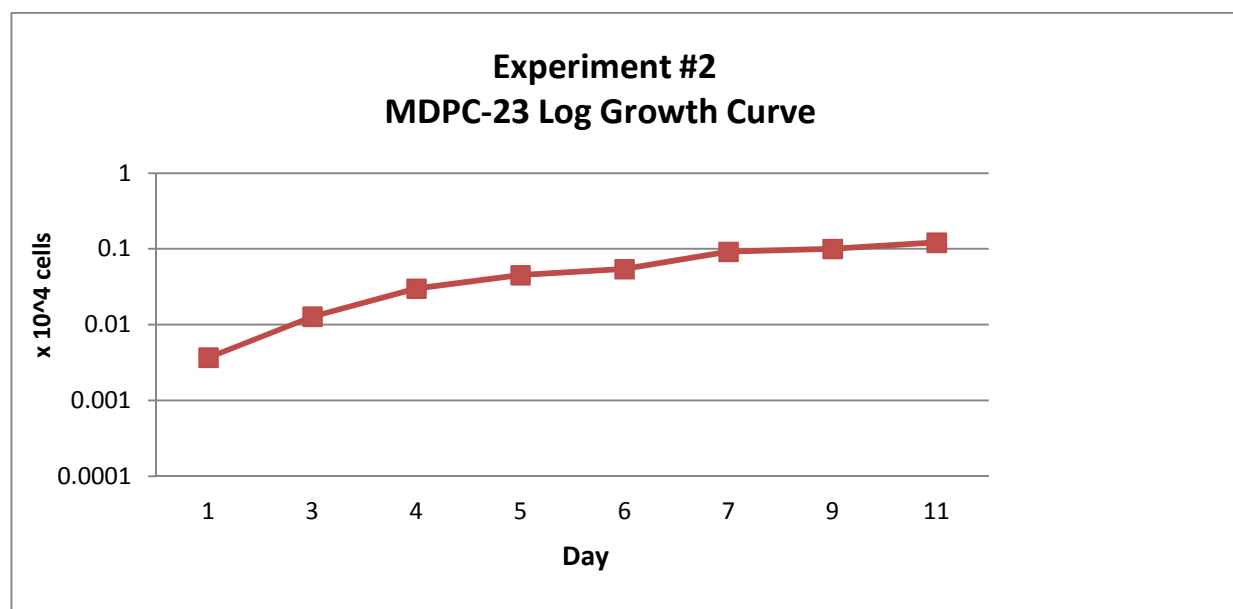


Figure 6: Experiment #2 MDPC-23 cell log growth curve during 11 days in cell culture manually counted.

The DNA standard curve for Experiment #2 was plotted from data obtained from the spectrofluorometer (Figure 7). Since a 96-well plate could only hold one half of the total number of samples, two standard curves were obtained corresponding to Samples Day 1-Day 5 and Day 6-11. The corresponding equations were used to calculate DNA concentration in ng/ml after subtracting background fluorescence and multiplying the concentration with the appropriate

dilution factor (Table 2). Samples from Day 6-Day 11 had a dilution factor of 20 due to the large number of cells at the later time points. Figure 8 shows MDPC-23 cell DNA content curve during 11 days in culture.

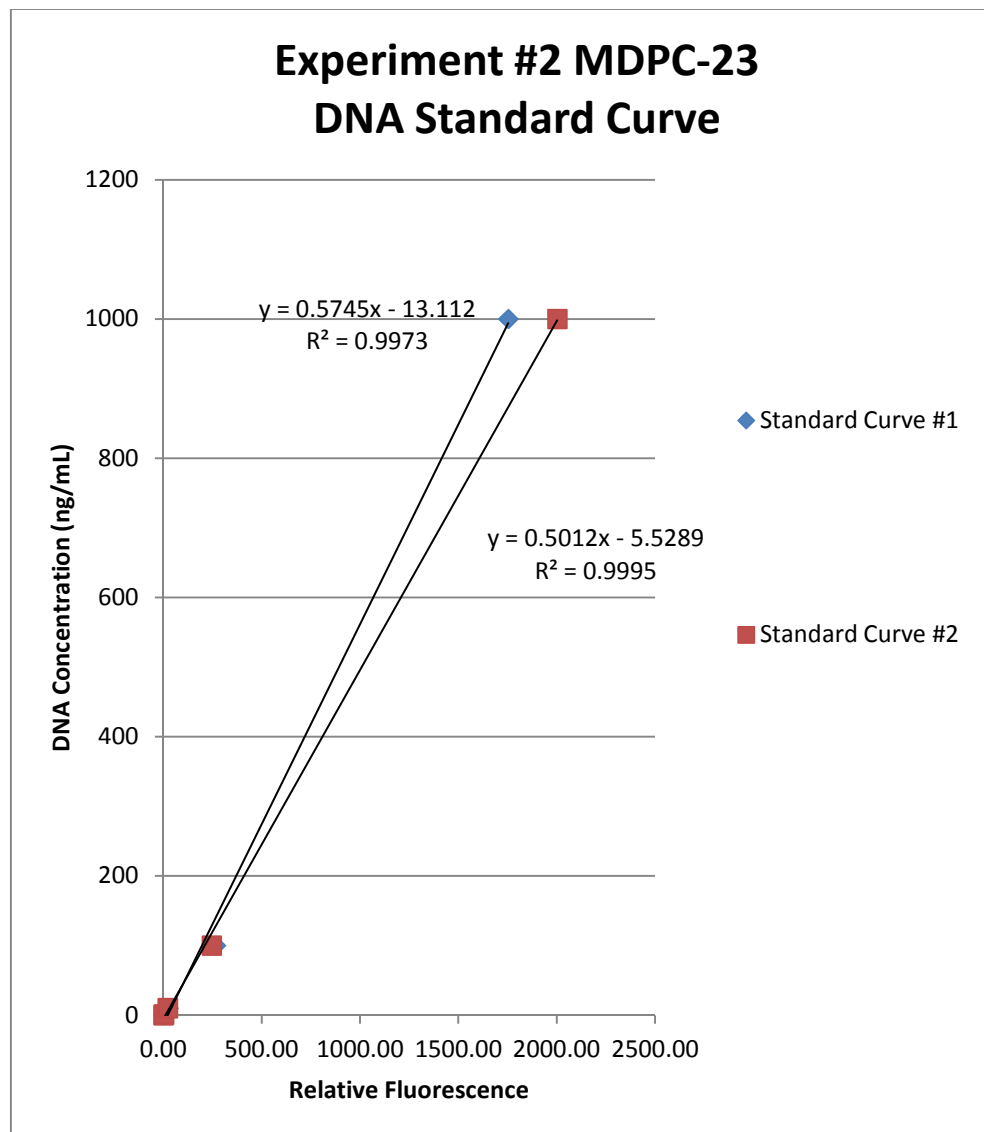


Figure 7: Experiment #2 DNA standard curves.

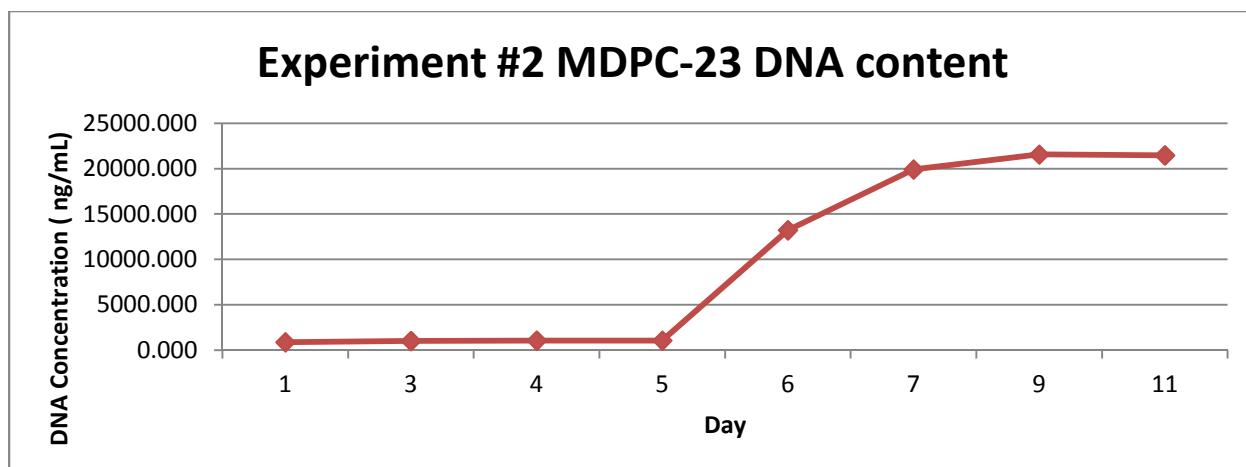


Figure 8: Experiment #2 MDPC 23 DNA content curve during 11 days in culture corresponding to Table 2 in the Appendix 1.

DNA concentration and cell numbers for Experiment #2 were compared as a function of time and they did not follow a similar trend (Figure 9). DNA concentration and cell numbers were then correlated producing a correlation coefficient of 0.875 (Figure 10).

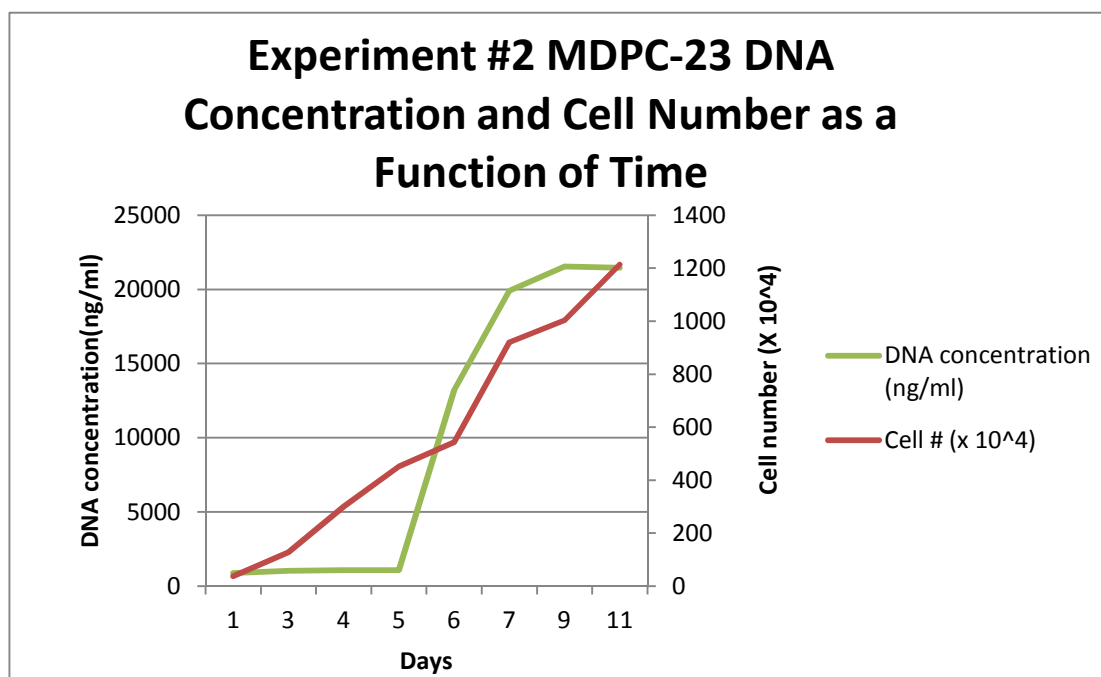


Figure 9: Experiment #2 MDPC-23 DNA concentration and cell number as a function of time after 11 days in culture.

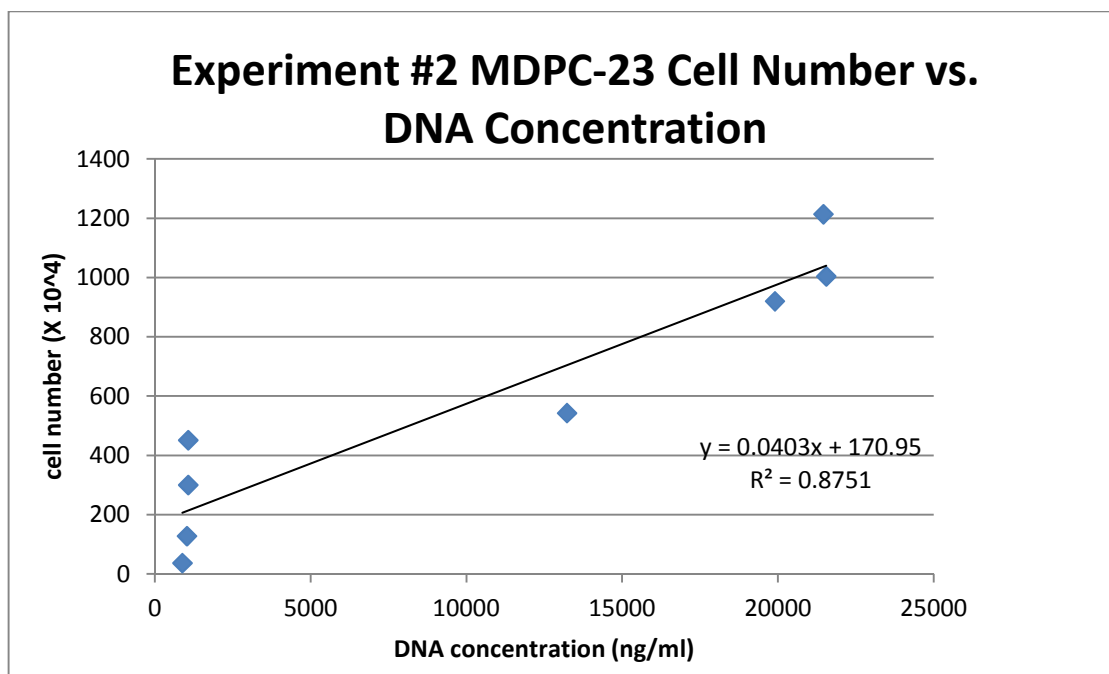


Figure 10: Experiment #2 MDPC-23 DNA concentration vs. cell number correlation.

The third experiment was done to correct the low correlation coefficient between the cell numbers and DNA content in the 2nd experiment and also to correct the inadequate dilution of the DNA samples for the DNA analysis. One strategy to achieve this was to dilute all samples in the same manner so that the dilution factor was consistent for all cell counts and also for DNA analysis. Experiment #3 MDPC-23 growth curve and its Log curve are shown in Figures 11 and 12. The cells in this experiment were counted using TC10™ Automated Cell Counter (BioRad).

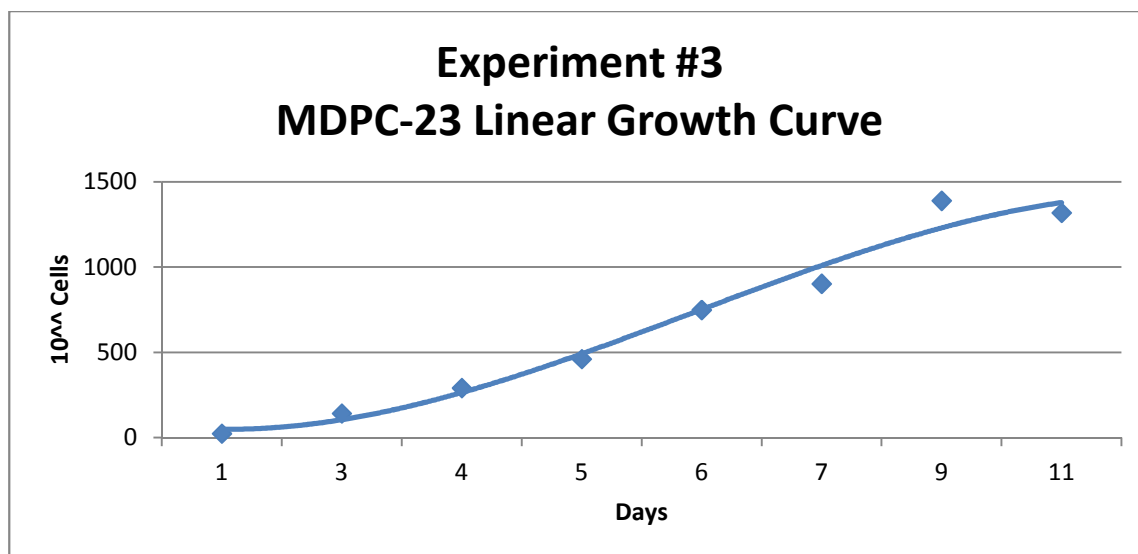


Figure 11: Experiment #3 MDPC-23 growth curve during 11 days in cell culture counted with TC10™.

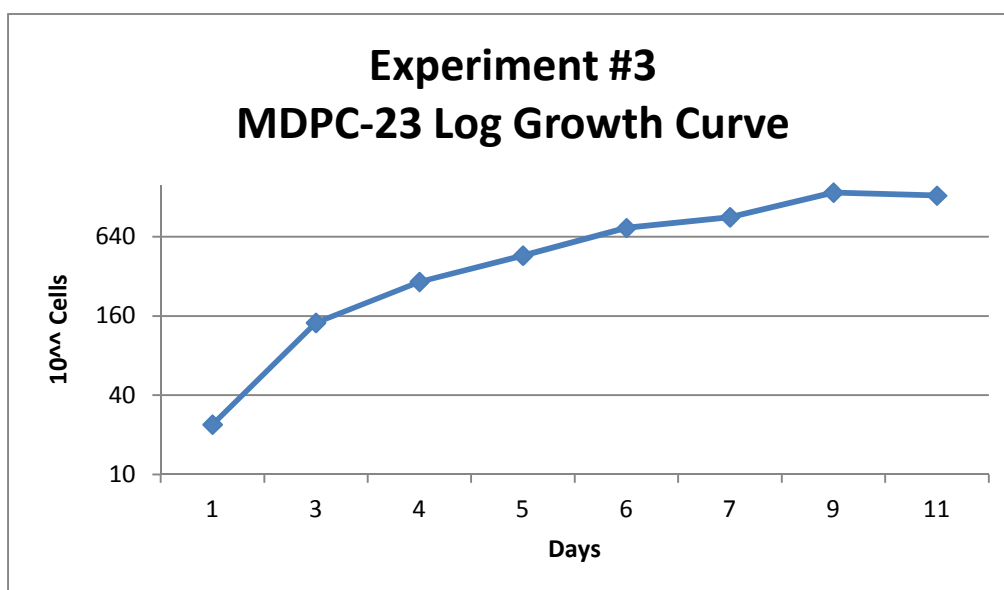


Figure 12: Experiment #3 MDPC-23 log growth curve during 11 days in cell culture counted with TC10™.

In Experiment #3, DNA standard curves were plotted and equations for standard curves 1 and 2 were used to calculate DNA concentration for each data point.

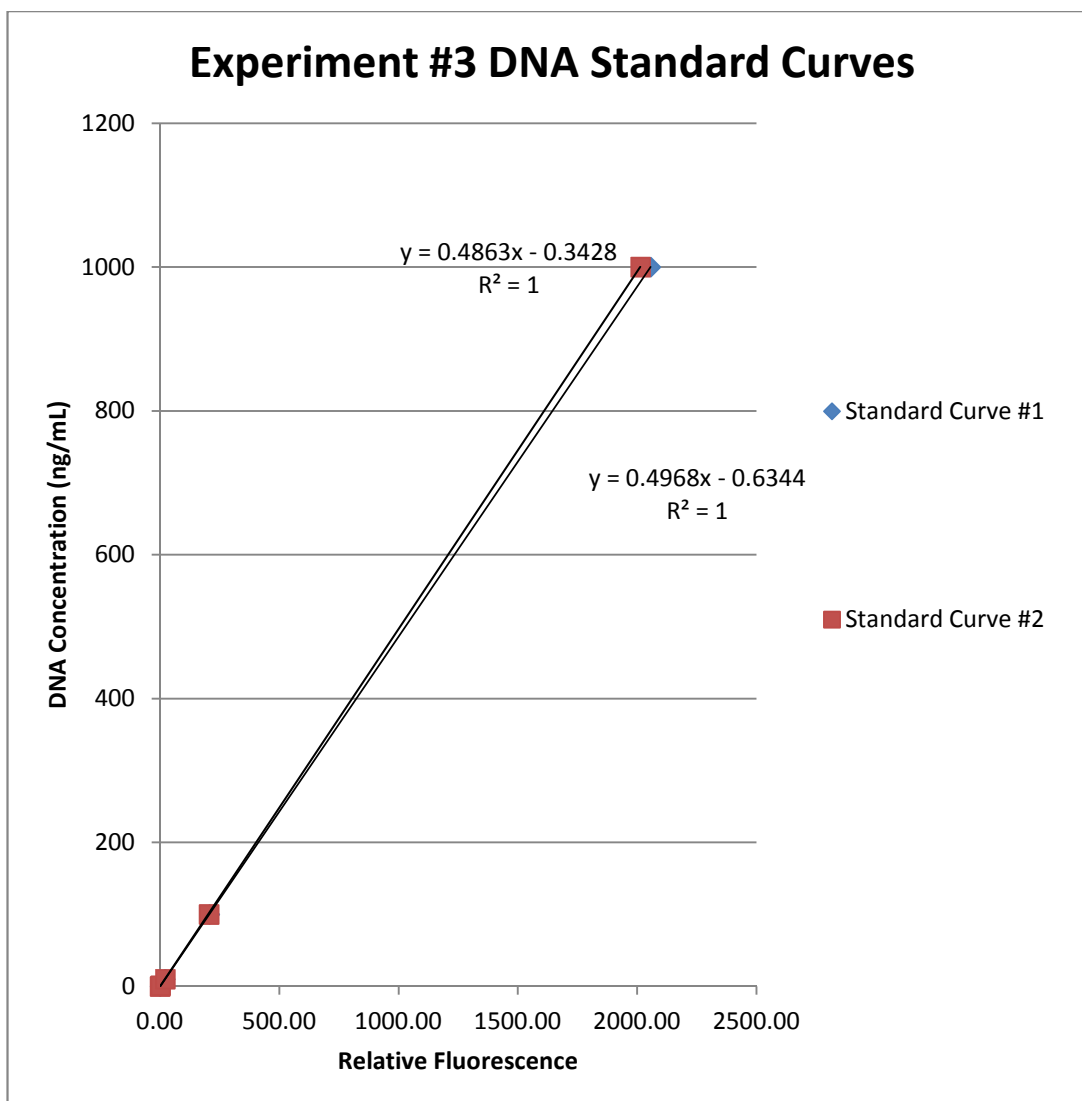


Figure 13: Experiment #3 DNA standard curves.

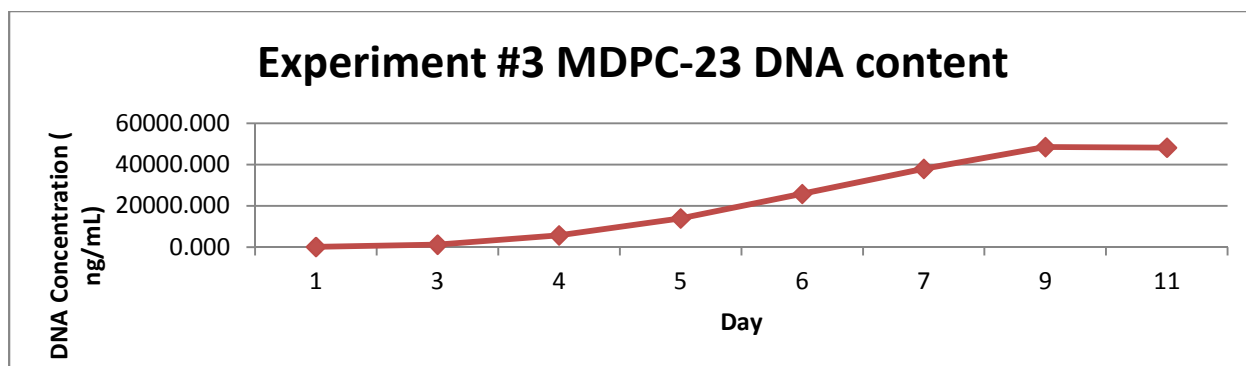


Figure 14: Experiment #3 MDPC-23 cell DNA content curve, after 11 days in culture corresponding to Table 3 in Appendix 1.

DNA concentration and cell numbers were then correlated as a function of time showing they both follow a very similar trend (Figure 15). Then, DNA concentration and cell numbers were correlated resulting in a high correlation coefficient of 0.981 (Figure 16).

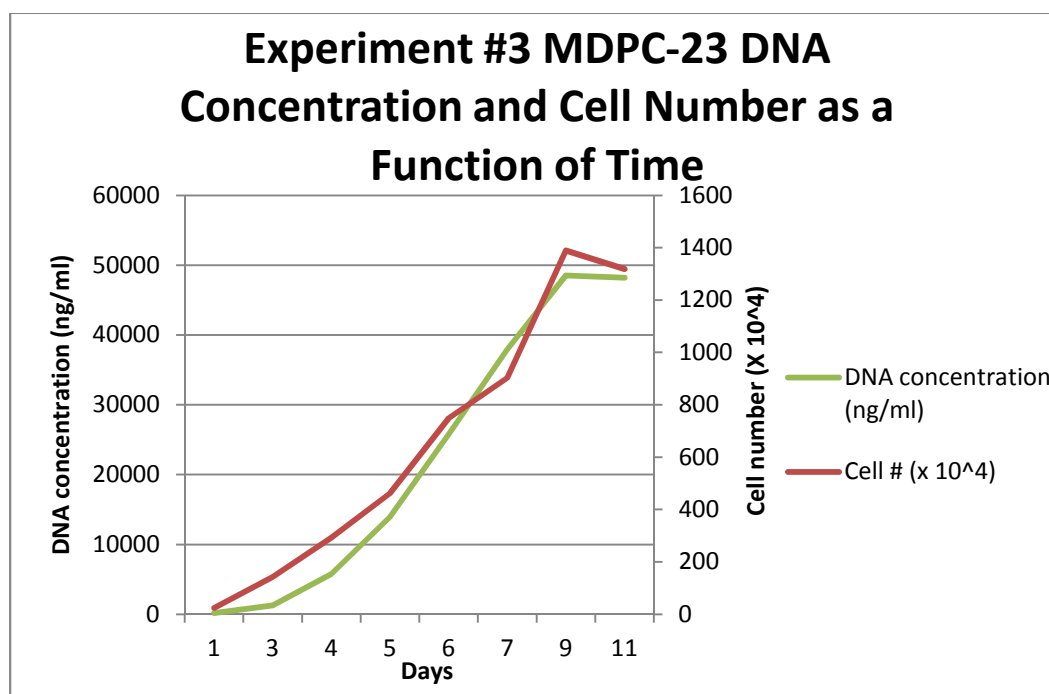


Figure 15: Experiment #2 MDPC-23 DNA concentration and cell number as a function of time after 11 days in culture.

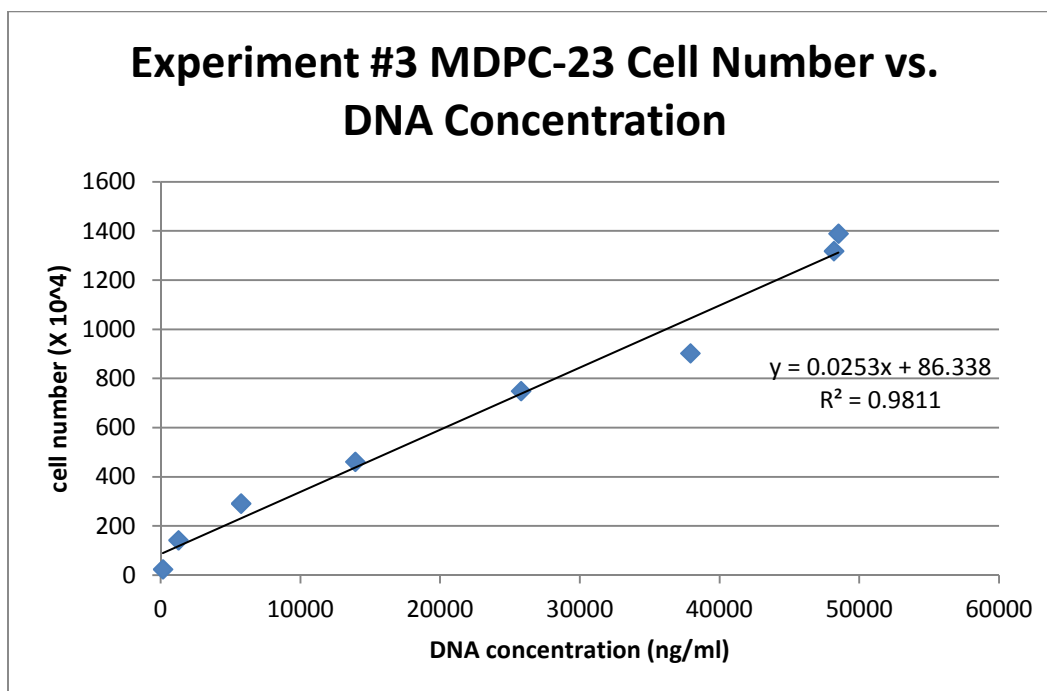


Figure 16: Experiment #3 MDPC-23 cell DNA concentration vs. cell number correlation.

6.0 Discussion

The growth curves of MDPC-23 cells in tissue culture have a typical S-shape when plotted on linear coordinates and a linear shape when plotted as log of cell number vs. time on a logarithmic scale. The growth curves have the standard appearance of logistic function with cells eventually tapering off in proliferation rate between day 7 and day 9. MDPC-23 cells reached confluence by day 3 but they kept proliferating with ample fresh media. Eventually cells did run out of space becoming a multilayer culture and thus their numbers tapered off. Some started dying at later time points as evident by cell counts using Trypan Blue dye. The cell numbers were plotted as both arithmetic and log curves depicting both linear and log relationships, respectively. The overall growth curve shape for MDPC-23 odontoblast-like cells in this experiment compares favorably with growth curves from an initial article on MDPC-23 cell line by Hanks et al. (1998).

Direct visual cell counting using a hemocytometer is an inexpensive simple method to determine cell numbers (Quent et al. 2010). Advantages of the hemocytometer are low cost, direct counting, no need for elaborate equipment and the ease of use. Disadvantages include need to obtain a single cell suspension per sample and there could be operator error and operator variability. It is also a time consuming effort. The cell suspension needs to be distributed uniformly to prevent clumping and skewing of the numbers.

Counting cells with the TC10™ automatic cell counter using capillary-filled disposable loading chambers removes subjectivity between users by applying algorithms to identify cells, disaggregate clusters and reject debris (Hefner et al., BioRad 2010). Automated cell counting has been shown to have smaller counting variation percentage when compared to hemocytometer counting (Hefner et al., BioRad 2010) and increased precision by eliminating human subjectivity

with the counting algorithm. The MDPC-23 cell growth curve for Experiment #3 when automatic cell counts were done appears more uniform and smoother as compared to Experiment #2 cell growth curve where cell counts were done manually (Figures 5 and 11, respectively).

The PicoGreen assay has its own advantages and disadvantages. PicoGreen cost is only 33 cents per test, it is dsDNA specific and is a very sensitive and highly reproducible test. A DNA standard is provided in the kit. Even though it has direct correlation with the cell number, by itself it can only approximate cell numbers. The disadvantages of using PicoGreen assay include signal quenching and need for using black plates as samples have to be protected from light (Quent et al. 2010). Signal quenching occurs due to short-range interactions between the fluorophore and its local environment (Invitrogen Molecular Probes® Handbook).

PicoGreen reagent can't penetrate cell membranes thus DNA must be released with a lysis reagent. Extracellular matrix proteins do not interfere with PicoGreen signals but salts like NaCl and MgCl₂ reduce fluorescence signals by 30%. Bovine serum albumin increases the fluorescent signal by 16% and phenol and triton X-100 increase signals by 13% and 7% respectively (Quent et al. 2010).

The cell doubling time, T_c, is the time it takes to complete a cell division cycle. In our experiment T_c (cell doubling time) varied somewhat from Experiment 1 through Experiment 3. These doubling times were then averaged, with an average cell doubling time of 0.996 +/- 0.095 days.

During the DNA quantification part of the study in Experiment #2, it was important to do a preliminary study to determine the correct dilution for later time point samples to ensure DNA amounts were within the limits of the standard curve. Figure #8 depicts the problem: with no dilution for early data points (Days 1, 3, 4 and 5) there is not much difference in the amount of

DNA found in the samples. In the later time points (Days 6, 7, 9, and 11) the dilution factor was not adequate (only 20X) and DNA concentrations were at the upper limit of the DNA standard curve and there was not much difference between the samples in the amount of the DNA. This problem was then corrected in Experiment #3 where dilutions were consistent throughout (80X dilution) enabling consistent data input and then output. Even though, theoretically, the dilution factor should be accounted for in the calculation, in this study, different dilution factors made a significant difference in the correlation coefficient between cell numbers and DNA content (Experiment #2 $R^2 = 0.875$ vs. Experiment #3 $R^2 = 0.981$).

The results in Experiment #3 show a very high correlation between the growth curves of MDPC-23 cell numbers and DNA content for the cells at specific time points (correlation coefficient is 0.981).

In the last experiment, Experiment #3, proliferation rates were increasing from Day 1 to Day 9, peaking at Day 9. At Day 11 there was a decrease in the total cell number. This could be due to cells running out of space and possibly even starting to die off. This is consistent with growth curve data in experiments by Pereira et al. (2012).

Clinical implications of this study have to do with the cell behavior with respect to proliferation rate. Proliferation rates of the MDPC-23 cell line would clinically impact the rate at which the odontoblast stem cells within the 3D geometric scaffold would undergo differentiation and mineral production and this would have an effect on the rate of maturation of the engineering scaffold *in vivo*.

The goal of this research was to lay the groundwork for further studies to involve MDPC-23 cell line in 2D scaffolds *in vitro* (Appendix 2) and then 3D biomaterial scaffold experiments *in vivo*. Here, biological activity of pulp stem cells within the biomaterial scaffold would

promote dental tissue regeneration while preserving tooth vitality when compared to traditional restorative approaches. Dentin regeneration could be used clinically when there is loss of tooth structure due to caries or in direct pulp capping procedures to stimulate dentin production around the dental pulp horn area thus preventing the need for root canal treatment if the cells themselves can repair the tooth. This approach, when successful, will change the way we manage and treat dental disease.

7.0 Conclusion

The typical S-shaped growth curve of the MDPC-23 cell line was confirmed.

The cell doubling time (T_c) for MDPC-23 for Experiment #1 growth curves was 1.02 days and 1.12 days. T_c for Experiment #2 was 0.94 days and for Experiment #3 was 0.90 days. The average cell doubling time for all 3 experiments was 0.996 ± 0.095 days.

The cell numbers and DNA content were found to be closely correlated with correlation coefficient of $R^2 = 0.98$.

This study confirmed the null hypothesis that MDPC-23 cell numbers can be accurately measured by DNA content. Growth curves determined by counting cell numbers and by measuring DNA content were comparable.

Proper dilutions applied evenly over all the samples made the difference in ensuring proper DNA content data input and then output.

Literature Cited

- Andreeff M, DW Goodrich, AB Pardee (2000). Chapter 2 Cell Proliferation, Differentiation, and Apoptosis. Holland-Frei Cancer Medicine 5th Edition
- Balic A, B Rodgers, M Mina (2009). Mineralization and expression of Colla1-3.6GFP transgene in primary dental pulp culture. *Cells Tissues Organs* 189:163-168
- Boyan BD, TW Hummert, DD Dean, Z Schwartz (1996). Role of material surfaces in regulating bone and cartilage cell response. *Biomaterials* 17:137-146
- Cordeiro MM, Z Dong, T Kaneko, Z Zhang, M Miyazawa, S Shi, AJ Smith, JE Nor (2008). Dental pulp tissue engineering with stem cells from exfoliated deciduous teeth. *J Endod* 34(8):962-969
- Dissanayaka WL, X Zhu, C Zhang, L Jin (2011). Characterization of dental pulp stem cells isolated from canine premolars. *J Endo* 37: 1074-1080
- Goldberg M, S Lacerda-Pinheiro, N Jegat, N Six, D Septier, F Priam, M Bonnefoix, K Tompkins, H Chardin, P Denbesten, A Veis, A Poliard (2006). The impact of bioactive molecules to stimulate tooth repair and regeneration as part of restorative dentistry. *Dent Clin N Amer* 50:277-298
- Guven EP, M E Yalvac, F Sabin, M M Yazici, A A Rizvanov, G Bayirli (2011). Effect of Dental Materials Calcium Hydroxide-containing Cement, Mineral Trioxide Aggregate, and Enamel Matrix Derivative on Proliferation and Differentiation of Human Tooth Germ Stem Cells. *JOE* 37(5) 650-656
- Hashimoto M, H Ohno, M Kaga, K Endo, H Sano, H Oguchi (2000). *In vivo* Degradation of Resin-Dentin Bonds in Humans over 1 to 3 Years. *J Dent Res* 79(6): 1385-91
- Invitrogen Molecular Probes® Handbook: Fluorescence Fundamentals
<http://www.invitrogen.com/site/us/en/home/References/Molecular-Probes-The-Handbook/Introduction-to-Fluorescence-Techniques.html>
- Kalajzic Z, P Liu, I Kalajzic, Z Du, A Braut, M Mina, E Canalis, DE Rowe (2002). Directing the expression of a green fluorescent protein transgene in differentiated osteoblasts: Comparison between rat Type I collagen and rat osteocalcin promoters. *Bone* 31(6): 654-660

- Kuhn LT, YL Liu, M Adcincula, YH Wang, P Maye, AJ Goldberg (2010). A nondestructive method for evaluating in vitro osteoblast differentiation on biomaterials using osteoblast-specific fluorescence. *Tissue Engineering* 16(6):1357-1366
- Liu H, S Gronthos, S Shi (2006). Dental pulp stem cells. *Methods in Enzymology* 419:99-113
- Ma PX Zhang R (2001). Microtubular architecture of biodegradable polymer scaffolds. *J Biomed Mater Res* 56:469-477
- Mina M, Braut A (2004). New insight into progenitor/stem cells in dental pulp using Colla1-GFP transgenes. *Cells Tissues Organs* 176:120-133
- Pereira LB, DT Chmello, MRW Ferreira, L Bachmann, AL Rosa, KF Bombonato-Prado (2012). Low Level Laser Therapy Influences Mouse Odontoblast-Like Cell Response *In Vitro*. *Protomedicine and Laser Surgery*. 30(4) 206-213
- Petersen PE (2009). Global policy for improvement of oral health in the 21st century-implications to oral health research of World Health Assembly 2007, World Health Organization Community. *Dent Oral Epidemiology* 37:1-8
- Petersen PE, T Yamamoto (2005). Improving the oral health of older people: The approach of the WHO Global Oral Health Programme. *Community Dent Oral epidemiology* 33:81-92
- Quent W MC, D Loessner, T Friis, JC Reichert, DW Hutmacher (2010). Discrepancies between metabolic activity and DNA content as tool to assess cell proliferation in cancer research. *J Cell Mol Med* 14(4): 1003-1013
- Ro A J, SJ Huang, RA Weiss(2008). Synthesis and Thermal Properties of Telechelic Poly(Lactic Acid) Ionomers. *Polymer* 49:422-431
- Roberts HW, JM Toth, DW Berzins, DG Charlton (2008). Mineral Trioxide Aggregate Material Use in Endodontic Treatment: A Review of Literature. *Dental Materials* 24: 149-164
- Rodriguez AP, H Tsujiwa, M Gunduz, B Cengiz, N Nagai, R Tamamura, S S Borkosky, T Takagi, M Inoe, H Nagatsuka (2009). Influence of the microenvironments on gene and protein expression of odontogenic-like and osteogenic-like cells. *Biocell* 33(1): 39-47
- Sloan AJ, RJ Waddington (2009). Dental pulp stem cells: What, where, how? *International J of Ped Dent* 19:61-70

- Srinivasan D, M Jayanthi (2011). Comparative evaluation of formocresol and mineral trioxide aggregate as pulpotomy agents in deciduous teeth. *Indian J Dent Res* 22 (3): 385-390
- Tay FR, DH Pashley. Dentin Bonding-Is There a Future? *Journal of Adhesive Dentistry* 6(4) 263
- Tonomura A, D Misuno, A Hisada, N Kuno, Y Ando, Y Sumita, M Honda, K Satomura, H Sakurai, M Ueda, H Kagami (2010) Differential effect of scaffold shape on dentin regeneration. *Annals of Biomedical Engineering* 38(4):1664-1671
- Tziafas D (2004) The future role of a molecular approach to pulp-dentinal regeneration. *Caries Res* 38:314-320
- Wang J, X Liu, ZX Jin, H MA, J Hu, L Ni, PX Ma (2010). The odontogenic differentiation of human dental pulp stem cells on nanoforous poly(L-lactic acid) scaffolds *in vitro* and *in vivo*. *Acta Biomaterialia* 6:3856-2863
- Wang Y, Y Liu, P Maye, D W Rowe (2006). Examination of mineralized nodule formation in living osteoblastic cultures using fluorescent dyes. *Biotechnol Prog* 22(6) 1697-1701
- Yao N, S Li, Y Jiang, S Qiu, Y Tan (2011). Amelogenin promotes odontoblast-like MDPC-23 cell differentiation via activation of ERK1/2 and p38 MAPK. *Mol Cell Biochem* 355: 91-97
- Yu G. J. Ji, J. Shen (2006). Synthesis and characterization of cholesterol-poly (ethylene glycol)- poly(D,L-lactic acid) copolymers for promoting osteoblast attachment and proliferation *J Mater Sci* 17: 899-909
- Yu G, K Ji, J Shen (2005). Cholesterol Tethered Poly(DL-lactic acid) for promoting osteoblast attachment and growth. *Journal of Bioactive and Compatible Polymers* 20: 527-540

Appendix 1

Samples									
Day	Sample Well	Fluorescence Readings			AVG Fluorescence	Background Subtraction	Calculated DNA Conc	xDilution Factor	AVG DNA Conc (ng/mL)
1	A	1370.27	1844.86	1719.84	1644.991	1638.621	928.276	928.276	
1	B	1486.09	1435.21	1192.95	1371.417	1365.047	771.107	771.107	
1	C	1747.18	1547.844	1671.16	1655.394	1649.024	934.252	934.252	877.879
3	A	1602.23	1914.056	2184.56	1900.280	1893.910	1074.939	1074.939	
3	B	1498	1548.338	1891.37	1645.902	1639.532	928.799	928.799	
3	C	1498.22	1887.261	2287.1	1890.858	1884.488	1069.527	1069.527	1024.422
4	A	1871.25	1605.799	1649.26	1708.766	1702.396	964.915	964.915	
4	B	2071.53	1879.085	2149.48	2033.366	2026.996	1151.397	1151.397	
4	C	1959.29	1705.546	2057.43	1907.422	1901.052	1079.042	1079.042	1065.118
5	A	1999.26	1896.129	2062.28	1985.889	1979.519	1124.122	1124.122	
5	B	2083.3	1898.371	2034.23	2005.300	1998.930	1135.273	1135.273	
5	C	1354.06	1564.011	2064.63	1660.900	1654.530	937.415	937.415	1065.603
6	A	1058.38	1036.469	1048.58	1047.808	1041.552	516.497	10329.939	
6	B	1493.52	1635.465	1534.67	1554.552	1548.295	770.477	15409.534	
6	C	1512.78	1264.084	1445.84	1407.566	1401.310	696.808	13936.153	13225.209
7	A	1954.05	1983.763	2019.18	1985.663	1979.407	986.550	19730.998	
7	B	1970.9	1971.932	2107.6	2016.811	2010.555	1002.161	20043.225	
7	C	1990.78	2003.971	2022.07	2005.607	1999.351	996.546	19930.913	19901.712
9	A	2084.01	2150.387	2115.66	2116.684	2110.428	1052.217	21044.349	
9	B	2193.83	2155.32	2288.84	2212.665	2206.409	1100.323	22006.466	
9	C	2182.01	2105.775	2229.49	2172.427	2166.170	1080.156	21603.113	21551.309
11	A	2126.93	2115.657	2180.77	2141.120	2134.864	1064.465	21289.295	
11	B	2184.11	2103.311	2173.88	2153.767	2147.511	1070.804	21416.072	
11	C	2196.41	2087.781	2252.6	2178.931	2172.675	1083.416	21668.316	21457.895

Table 3: Experiment #2 MDPC 23 DNA content samples data corresponding to Figure 7.

Samples									
Day	Sample Well	Fluorescence Readings			AVG Fluorescence	Background Subtraction	Calculated DNA Conc	xDilution Factor	AVG DNA Conc (ng/mL)
1	A	10.534	11.271	11.735	11.180	4.959	2.069	165.501	
1	B	11.288	10.752	10.814	10.951	4.730	1.958	156.605	
1	C	9.947	11.196	10.857	10.667	4.446	1.819	145.530	155.879
3	A	34.067	31.522	33.123	32.904	26.683	12.633	1010.651	
3	B	36.395	36.767	35.914	36.359	30.138	14.313	1145.052	
3	C	53.080	48.140	46.508	49.243	43.022	20.579	1646.291	1267.331
4	A	133.462	125.965	114.258	124.562	118.341	57.206	4576.501	
4	B	156.058	158.348	150.014	154.807	148.586	71.914	5753.153	
4	C	183.235	182.247	189.027	184.836	178.615	86.518	6921.427	5750.360
5	A	321.601	330.034	318.776	323.4703333	317.249	153.936	12314.844	
5	B	364.469	368.489	350.334	361.097	354.876	172.234	13778.685	
5	C	414.743	409.166	407.043	410.317	404.096	196.169	15693.540	13929.023
6	A	673.337	688.464	694.457	685.419	679.659	337.020	26961.629	
6	B	613.624	660	652.074	641.899	636.139	315.400	25231.970	
6	C	626.401	647.576	647.406	640.461	634.701	314.685	25174.805	25789.468
7	A	908.544	898.091	891.222	899.286	893.526	443.269	35461.532	
7	B	976.501	971.502	1007.733	985.245	979.485	485.974	38877.913	
7	C	994.894	1017.039	983.023	998.319	992.559	492.469	39397.500	37912.315
9	A	1264.968	1276.87	1294.962	1278.933	1273.173	631.878	50550.249	
9	B	1231.686	1223.218	1235.912	1230.272	1224.512	607.703	48616.253	
9	C	1184.432	1162.740	1172.758	1173.310	1167.550	579.404	46352.355	48506.286
11	A	1228.921	1232.398	1233.026	1231.448	1225.688	608.288	48663.005	
11	B	1248.58	1239.801	1249.737	1246.039	1240.279	615.536	49242.910	
11	C	1180.628	1166.082	1195.084	1180.598	1174.838	583.025	46642.009	48182.641

Table 4: Experiment #3 MDPC 23 DNA content samples data corresponding to Figure 11.

Appendix 2

Future Steps:

Dewetting for Texture

Our goal for future research would involve dewetting of the thin films. In a tissue engineering system, cell behavior is strongly influenced by the surface properties of the biomaterial, including surface charge, chemistry and topography (Boyan et al. 1996). The goal in synthetic scaffold preparation is for undifferentiated cells to attach, proliferate and differentiate into the desired tissue type. Dewetting/crystallization of thin films can produce a textured surface and can be used for nano-scale surface tissue engineering. Nano-scale topography is important in the extracellular matrix and cell signaling.

Dewetting of thin polymer films is a dynamic process which depends on energies between polymer/air or polymer/substrate. Initially polymer is spin coated onto the substrate. When the polymer spreads over the substrate surface, the solvent evaporates leaving behind glassy polymer. The film attains equilibrium when it is heated above T_g (glass transition temperature) while dewetting the surface due to pressure gradient forming due to thermally induced thickness fluctuations. In the case of semi-crystalline polymers, surface formation is governed by both dewetting and by crystallization. On cooling below T_m (melting temperature), crystallization can arrest dewetting and dominate film morphology.

Scaffolds play a crucial role in three-dimensional new tissue formation (Ma et al. 2001). Polylactic acid (PLA) is a biocompatible and cytocompatible polymer scaffold with a long history of use in medical devices. Proteins from cell culture media help cells adsorb onto PLA surfaces. Bioactive functional groups attached to the PLA membrane promote cell attachment

and function. Polymers such as PLA are non-immunogenic, non-toxic and bioresorbable (Ma et al. 2001). They are convenient as solid phase scaffolds or as injection and polymerization solutions at the site of damage (Bonzani et al. 2006).

Unmodified PLA surfaces display poor adhesion and cell growth (Yu et al. 2005). Thus, PLA can be chemically modified (Ro et al. 2008) with itaconic anhydride and neutralized with Li acetate to prepare telechelic PLA ionomers. The incorporation of ions onto a surface was previously shown to change the adsorption of proteins and thus the cell binding process (Boyan et al. 1996). It may be possible to functionalize the PLA with a range of biomolecules like cholesterol useful for controlling cell responses.

Cholesterol- PLA

Cholesterol is a fat soluble amphiphilic molecule that plays a very important role in eukaryotic cell membranes. Cholesterol stabilizes membrane receptors that influence important and complex pathways for biosynthesis, efflux, uptake and molecular transport. Cholesterol makes fluid membranes more rigid, thus reducing passive permeability of molecules and increasing mechanical durability of the lipid bilayer (Hwang et al., 2002).

Figure 17: Chemical structure of cholesterol as adopted from Zhou et al. 2009:

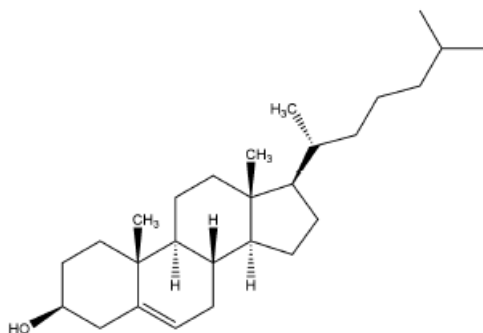
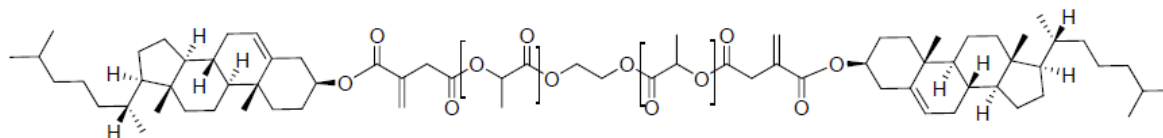


Figure 18: Cholesterol encapped PLA structure as adapted from Zhou et al. 2009



Cell behavior can be influenced by cholesterol modified PLA surfaces (Ye et al. 2005). Cell attachment, proliferation, cell activity and cell morphology have been studied in bone tissue engineering (Yu et al. 2005 and Yu et al. 2006) but not in dentin tissue engineering. Thus, MDPC-23 cell line behavior will be studied on PLA and Cholesterol-PLA surfaces.

Cell Culture Differentiation Assay

The influence of the coated discs on differentiation will be evaluated with an *in vitro* culture of MDPC-23 cells. The cells will be seeded onto 6-well plates, cultured to 70% confluence and incubated in the induction medium (10nmol/l dexamethasone, 10mmol/l beta-glycerophosphate, 50ug/ml L-ascorbic acid phosphate, 10nmol/L 1,25 dihydroxyvitamin D3 and 10% FBS) for 1-4 weeks and stained with xylene orange to check for mineral production.

Since alkaline phosphatase (ALP) is considered an early osteogenic marker, after 1 week of induction cells will be fixed and stained for ALP (Sigma-Aldrich, Steinheim, Germany). After 2 weeks of induction cells will be analyzed by immunofluorescence for DSPP expression. After 4 weeks, cells will be fixed with 60% isopropanol for 20 min and stained for mineralization with 2% alizarin red stain.

Preparation of Thin PLA and Cholesterol-PLA Films

The process of fabrication of cholesterol-PLA (Ch-PLA) films was performed and described by Rubinder Kaur Lakhman, Graduate Research Assistant, Polymer Program, Institute of Materials Science at University of Connecticut, Storrs.

Poly(lactide), PLA (M_w 148770, T_g 59.24°C, T_M 165.88°C) was obtained from NatureWorks LLC. Cholesterol end-functionalized PLA (Ch-PLA) was synthesized using ring opening polymerization methods to give a narrow molecular weight distribution polymer using $SnOct_2$ as the catalyst and cholesterol as the initiator. Cholesterol and L-lactide are dried overnight in vacuum oven to remove traces of water. L-lactide, 2.592g (0.018 mol), cholesterol, 386mg (0.001 mol), and $SnOct_2$, 6mg (0.014 mmol) are taken up in a dried Schlenk tube equipped with a stir bar. The Schlenk tube is degassed by applying a vacuum for 30 mins, followed by purging with nitrogen. This is repeated three times to ensure high vacuum in the Schlenk tube which is then immersed in an oil bath maintained at 150 °C. The reaction proceeds for 12h and the solid product is dissolved in dichloromethane followed by precipitation in cold methanol. The final product is obtained by filtration and drying in a vacuum oven overnight.

Films were prepared by spin coating a polymer solution on glass coverslips using SCS Corp., Model P6700 spin coater. The glass coverslips were washed several times by immersion and sonication, first in soap solution and then in distilled water for 20 minutes each time. The discs were air dried and stored in covered polystyrene petri dishes. A 1% w/v solution of ChPLA (-or C-PLA) in chloroform was spin coated onto a clean coverslip using a rotor speed of 3000rpm for 80 seconds.

Mineral Detection in Cell Culture on TCP, PLA and Cholesterol-PLA disks

The cholesterol coated PLA discs will be sterilized under UV light for 1 hour. The MDPC-23 cells will be plated onto TCP (control), PLA and Cholesterol-PLA disks at a density of 15,000 cells/cm² and cultured in mineralization solution containing 100ug/ml ascorbic acid, 10mM β -glycerophosphate and 10nM dexamethasone and incubated at 37°C and 5% CO₂ for 14 days in 6-well plates. At 14 days and 21 days the discs will be imaged with a microscope (Olympus IX50 inverted microscope) for mineralization nodules (Yao et al. 2011) after being stained with von Kossa stain.

The common methods to visualize mineral in cell culture include von Kossa (VK) staining and alizarin red S (ARS) staining. In both methods, cells need to be fixed prior to staining, thus terminating the culture (Wang et al. 2006).

Von Kossa method is a non-specific Ca binding reaction, where silver ions bind anions of calcium salts (phosphates, sulfates, carbonates). Silver salts are then reduced to produce dark brown/metallic black silver staining. When doing von Kossa staining cells are fixed with 4% paraformaldehyde in neutral buffer for 15min, washed with distilled water and then treated with 1% AgNO₂ for 1hr, washed again in distilled water and treated with 2.5% sodium thiosulfate for 5 minutes. The specimens are then examined under the light microscope (Yao et al 2011.) . Another way to do von Kossa staining is to fix cells in cold methanol for 15-20min and after rinsing the fixed plates are incubated with 5% silver nitrate under UV light using 2 cycles of auto-crosslink (1200mjoules X 100) in a UC Stratalinker (Stratagene, La Jolla, CA). Mineralized nodules are dark brown or black spots (Wang et al. 2006).

Alizarin red S stain reacts specifically with calcium cations to form a chelate. For alizarin red S (Sodium alizarin sulfonate) staining, 2% alizarin red S (Sigma) is prepared in distilled

water and pH adjusted to 4.1-4.3 using 0.5% ammonium hydroxide. Cells are fixed with 10% formalin (15 min), washed and stained with alizarin red S for 10-15min. Then, the cells are rinsed with distilled water and red spots are noted (Wang et al. 2006).

Two new methods that don't require cell line termination are xylenol orange (XO) and calcein blue. Xylenol orange ($C_{31}H_{28}N_2O_{12}SNa_4$) and calcein blue ($C_{15}H_{15}NO_7$) are both calcium-chelating fluorochemicals that have specific excitation and emission wavelengths (xylenol orange 440/570 and 610nm and calcein blue 375 and 435 nm). Xylenol orange emits red fluorescent color in the fluorescent microscope using TRITC Red filter (Chroma Technology, Rockingham, CT), while calcein blue emits blue fluorescent color viewed with a Sapphire GFP filter (Chroma Technology).

Xylenol orange can be added to living cells *in vitro* to mark the mineralized products of cells. XO produces a red color when visualized under the microscope using a TRITC filter. XO powder will be dissolved in distilled water and filtered to make concentrated 20mM stock solution and stored at 4°C. XO can be added to living cells to a final concentration of 20mM for 4 hrs to overnight. XO-containing media can be replaced with fresh medium prior to photography to avoid fluorescent background at day 14 and day 21.

Calcein blue powder (Sigma) is dissolved in 100mM KOH (diluted in distilled water) and filtered to make 30mM stock solution, making sure the final concentration in culture media is 30uM (Wang et al 2006). These concentrations of XO and calcein blue (20uM XO and 30uM for CB) don't alter cell viability, DNA content or mineralization in the cell cultures. In addition, CB and XO can be used sequentially to distinguish old and new mineral deposition as shown previously by Wang et al. (2006).